13th World Conference on Earthquake Engineering
Vancouver, B.C., Canada
August 1-6, 2004
Paper No. 2721

ACTIVE STRUCTURAL CONTROL OF CONCRETE STRUCTURES FOR EARTHQUAKE EFFECTS

Mohammad SHOOSHTARI[1] and Murat SAATCIOGLU[2]

SUMMARY

A method is presented for active control of reinforced concrete (R/C) structures against seismic excitations. An important aspect of the method presented is the extension of control process into the inelastic range of deformations. Computer software was developed for dynamic inelastic analysis of reinforced concrete structures, including the effects of control forces, illustrating the significance of active control analytically. This necessitated the formulation of stiffness matrix K as a function of time. Hysteretic behavior is modeled following the rules proposed by Takeda et al.[1]. The effects of instantaneous optimal control algorithms were investigated on structural response. Numerical examples were solved to illustrate the process of active structural control for R/C frame structures. The significance of the arrangement of control forces is presented. The results indicate that seismic response of an R/C structure can be reduced significantly with active control. There is an optimum combination of control forces and lateral displacements that can be established through dynamic analysis prior to application in practice.

INTRODUCTION

Behavior of structures during recent earthquakes has demonstrated that significant damage can be imposed on structures that are not designed on the basis of seismic design provisions of current building codes. Unfortunately, these structures constitute the majority of building and bridge stocks in the world. Therefore, seismic retrofitting has gained importance in recent years to reduce seismic vulnerability of existing structures. Among the options considered for seismic rehabilitation, a new approach has been emerging as a new technology for seismic risk mitigation. This technique involves active control of structural response during seismic excitations.

Seismic structural control includes the computation of control forces during an actual seismic event and the application of these forces to reduce or minimize the effects of earthquakes. Two seismic response quantities gain importance in structural control; i) lateral drift and ii) earthquake forces. Both of these response quantities are affected significantly by inelasticity, which is unavoidable in reinforced concrete

[1]PhD Candidate, Dept. of Civil Engineering, University of Ottawa, Ottawa, Canada, K1N 6N5.
[2]Professor and University Research Chair, Dept. of Civil Engineering, Univ. of Ottawa, Ottawa, Canada, K1N 6N5. E-mail:murat@eng.uottawa.ca

structures under strong earthquakes. The main objective of the research work presented in this paper is to develop a new method of active structural control applicable to R/C frame structures responding in the inelastic mode of deformations. A rotational spring is created at that end of a member upon yielding. The M-θ relationship, which follows the rules proposed by Takeda [1], establishes the stiffness of the spring. Instantaneous Optimal Control algorithms, including closed-loop, open loop and closed-open-loop processes incorporate active structural control.

EQUATION OF MOTION

The equation of motion of an *n* degree-of-freedom system, subjected to ground excitations and control forces, can be written as shown below:

$$Ma + Cv + Ku = Ea_g(t) + Df_c(t) \tag{1}$$

where, *M*, *C* and *K* are mass, damping and stiffness matrices, respectively; a_g and f_c are vectors which determine ground acceleration and control force; and *a*, *v* and *u* are response acceleration, velocity and displacement, respectively. Matrix *E* represents the degree of freedom in which the ground acceleration is applied, and matrix *D* shows the location of control forces. The ordinary solution of the differential equation given in Eq. (1) involves the introduction of a function to reduce the order of equation [2,3]. Accordingly, function *Z* can be introduced to reduce the order of equation and change the equation as shown below:

$$\dot{Z}(t) = AZ(t) + W_1 a_g(t) + Bf_c(t) \tag{2}$$

where:

$$Z(t) = \begin{bmatrix} u(t) \\ v(t) \end{bmatrix} \quad \dot{Z}(t) = \begin{bmatrix} v(t) \\ a(t) \end{bmatrix} \quad A = \begin{bmatrix} 0 & I \\ -M^{-1}K & -M^{-1}C \end{bmatrix} \quad W_1 = \begin{bmatrix} 0 \\ M^{-1}E \end{bmatrix} \quad B = \begin{bmatrix} 0 \\ M^{-1}D \end{bmatrix} \tag{3}$$

The solution of Eq. (2) leads to:

$$Z(t) = T[d(t - \Delta t) + \frac{\Delta t}{2} m(t)] \tag{4}$$

where:

$$d(t - \Delta t) = e^{\Delta t \Omega} T^{-1} \{ Z(t - \Delta t) + \frac{\Delta t}{2} [Bf_c(t - \Delta t) + W_1 a_g(t - \Delta t)] \}$$

$$m(t) = T^{-1} [Bf_c(t) + W_1 a_g(t)] \qquad \Omega = T^{-1} AT \tag{5}$$

T is a matrix whose columns are eigenvector of matrix *A*. The stiffness matrix *K* in above equations remains constant for all steps of time and is not suitable for the investigation of inelastic response. Therefore, the above approach has been modified to permit the local stiffness matrix *k* to change upon yielding. This makes the resulting global stiffness matrix *K* to become time-dependent, and necessitates a different approach in which matrix n(t) is introduced as shown below:

$$\dot{Z}(t) = A_1 Z(t) + W_1 a_g(t) + Bf_c(t) + n(t) \tag{6}$$

where:

$$A_1 = \begin{bmatrix} 0 & I \\ 0 & -M^{-1}C \end{bmatrix} \quad n(t) = \begin{bmatrix} 0 \\ -M^{-1}F_S(t) \end{bmatrix}$$

$$F_S(t) = F_S(t - \Delta t) + K(t)[u(t) - u(t - \Delta t)] \tag{7}$$

The solution of Eq. (6) is similar to that presented earlier:

$$Z(t) = T_1 [\, d_1(t - \Delta t) + \frac{\Delta t}{2} m_1(t)]$$

(8)

where:

$$d_1(t - \Delta t) = e^{\Delta t \Omega_1} T_1^{-1} \{ Z(t - \Delta t) + \frac{\Delta t}{2} [\, Bf_c(t - \Delta t) + W_1 a_g(t - \Delta t) + n(t - \Delta t)]\}$$

$$m_1(t) = T_1^{-1} [\, Bf_c(t) + W_1 a_g(t) + n(t)]$$

$$\Omega_1 = T_1^{-1} A_1 T_1$$

(9)

T_1 is a matrix whose columns are eigenvector of matrix A_1. The above method is applicable to the evaluation of both elastic and inelastic structural response.

Local stiffness matrix

When bending moment at the end of a flexural member reaches yield moment M_y, the behavior changes, and the member develops an inelastic region. Subsequently, a plastic hinge is created within this region whose properties can be represented by a rotational spring. The stiffness of the rotational spring is modeled analytically. For reversed cyclic loading, a hysteretic model is assigned to the spring, through which the stiffness values during various stages of loading, unloading and reloading are computed based on the rules of the model.

Typically, a frame member is modeled by two springs, one at each end. This is shown in Figure 1, where k_a and k_b are spring stiffnesses at member ends.

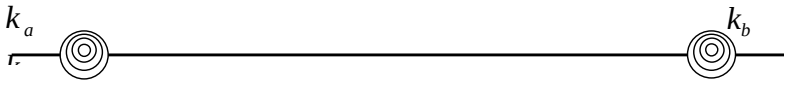

Figure 1 Element model with inelastic springs at member ends

These rotational springs are assigned a very high value until yielding, and hence do not rotate. Upon yielding, the spring stiffness changes and follows the rules of the hysteretic model selected.

If two parameters, S_a and S_b, are introduced as specified below;

$$S_a = \frac{k_a L}{4EI} \qquad\qquad S_b = \frac{k_b L}{4EI}$$

(10)

then, the local stiffness matrix of a member can be expressed as shown below, which is a symmetric matrix.

$$k = \alpha \begin{bmatrix} \frac{AL^2}{I} & 0 & 0 & -\frac{AL^2}{I} & 0 & 0 \\ & 12S_1 & 6LS_2 & 0 & -12S_1 & 6LS_4 \\ & & 4L^2 S_3 & 0 & -6LS_2 & 2L^2 S_5 \\ & & & \frac{AL^2}{I} & 0 & 0 \\ & Sym & & & 12S_1 & -6LS_4 \\ & & & & & 4L^2 S_6 \end{bmatrix}$$

(11)

Where:

$$\alpha = \frac{EI}{L^3} \qquad S_1 = \frac{1}{2S}(S_a + S_b + 4S_a S_b) \qquad S_2 = \frac{S_a}{S}(1+2S_b)$$

$$S_3 = \frac{S_a}{2S}(3+4S_b) \qquad S_4 = \frac{S_b}{S}(1+2S_a) \qquad S_5 = \frac{2}{S}(S_a S_b)$$

$$S_6 = \frac{S_b}{2S}(3+4S_a) \qquad S = 2(1+S_a)(1+S_b) - \frac{1}{2} \tag{12}$$

EI and *EA* are flexural and axial rigidities, respectively, and *L* is member length. The above formulation was adopted from Holzer [4].

Spring stiffness

Spring stiffness provides a relationship between bending moment and chord rotation. The chord rotation is the angle between the tangent at the end of a member and the line which joins the member end to the inflection point, as illustrated in Figure 2. The spring stiffness follows the rules of the hysteretic model when subjected to reversed cyclic loading.

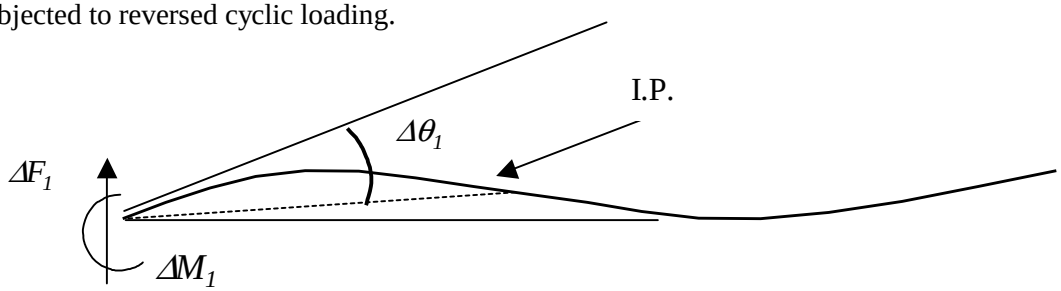

Figure 2 Illustration of a member in double curvature and a chord angle

The following ratio of incremental end moment, ΔM_1 to incremental chord rotation, $\Delta\theta_1$ is applicable prior to yielding.

$$\frac{\Delta M_1}{\Delta\theta_1} = \frac{3EI}{L_1} \tag{13}$$

L_1 in the above equation represents the distance between member end and the inflection point (shear span). A ratio of the initial elastic stiffness may be assigned to the post-yield stiffness, consistent with the assumption of constant post-yield stiffness of a bi-linear primary moment-rotation relationship. This ratio is defined as "h", leading to a post-yield stiffness of $3EIh/L_1$. This translates into the spring stiffness shown below.

$$k_a = \frac{3EI}{L_1} \times \frac{h}{1-h} \tag{14}$$

Eq. 14 is employed for all time steps of analysis, including the elastic response, for which h = 1.0, resulting in infinite spring stiffness for k_a.

Control force

Among the control algorithms utilized in Civil Engineering "Instantaneous Optimal Algorithm" is adopted here for the control force. In this algorithm, the performance index $J_1(t)$ is minimized. $J_1(t)$is introduced as explained below.

$$J_1(t) = z^T(t) Q z(t) + f_c{}^T(t) R f_c(t) \tag{15}$$

Where Q and R are the weighting matrices and are defined below:

$$Q = \begin{bmatrix} c \times K & 0 \\ 0 & c \times K \end{bmatrix} \qquad R = \begin{bmatrix} r & 0 & . & 0 \\ 0 & r & . & 0 \\ . & . & . & . \\ 0 & 0 & . & r \end{bmatrix} \tag{16}$$

For the optimization process, the Hamiltonian H is obtained as:

$$H = z^T(t) Q z(t) + f_c{}^T(t) R f_c(t) + \lambda^T [\, z(t) - T_1 d_1(t - \Delta t) - \frac{\Delta t}{2} (B f_c(t) + W_1 a_g(t) + n(t))] \tag{17}$$

Where, λ is the Lagrange multiplier vector. Eq. 17 is a modified version of the expression used by Lin et.al [5] and Soon [6], where the modification was made to introduce inelasticity into the stiffness matrix. The following conditions are met to minimize the performance index $J_1(t)$:

$$\frac{\partial H}{\partial z} = 0 \qquad \frac{\partial H}{\partial u} = 0 \qquad \frac{\partial H}{\partial \lambda} = 0 \tag{18}$$

Three methods can be employed for the solution of the algorithm, depending on the governing parameter for the control force. These methods are listed below:

1 - *Open-Loop Control Method*, where λ is only a function of ground excitation.

2 - *Closed-Loop Control Method*, where λ is only a function of feedback response.

3 - *Open-Closed-Loop Control Method*, where λ is a function of both ground excitation and feedback response. Analyses of structures presented in this paper are based on the Open-Loop Control Method.

APPLICATION OF SEISMIC STRUCTURAL CONTROL

The application of the above procedure is illustrated through two examples. The examples consist of a three-story and a five-story reinforced concrete building frames, each having different arrangements of control forces.

Three-Story Reinforced Concrete Frame Structure

A three-storey concrete building was designed using the provisions of the National Building Code of Canada [7]. A typical floor plan is illustrated in Figure 3(a). The frames in the short direction were modeled as shown in Figures 3(b), 3(c) and 3(d), with three different arrangements of control forces. The control forces were applied through actuators placed on floor slabs and prestressing strands attached to beam column joints, diagonally. The cables were capable of applying diagonal tension only, as tie members, without the capability of acting as compression struts. Pattern 1, shown in Figure 3(b), was intended to transform the interior bay to a bracing element along the height, similar to the effect of a shear wall. Pattern 2 was intended to control lateral deformations within the critical first storey to minimize damage to the first-storey columns. Pattern 3 shows an asymmetric control, where the entire frame is braced along one of the diagonals, while providing control for inter-storey drift in the opposite direction within individual bays.

The optimization of control force is dependent on the ratio of c and r parameters used in Eq. 16 in defining the weighting matrices Q and R. The c/r ratio establishes a critical balance between the level of displacement to be controlled and the magnitude of force required for such control. While maximizing the reduction in lateral displacement is desirable, this may require excessive control forces that may not be realized with the hardware available, or that may potentially create local anchorage and/or construction problems.

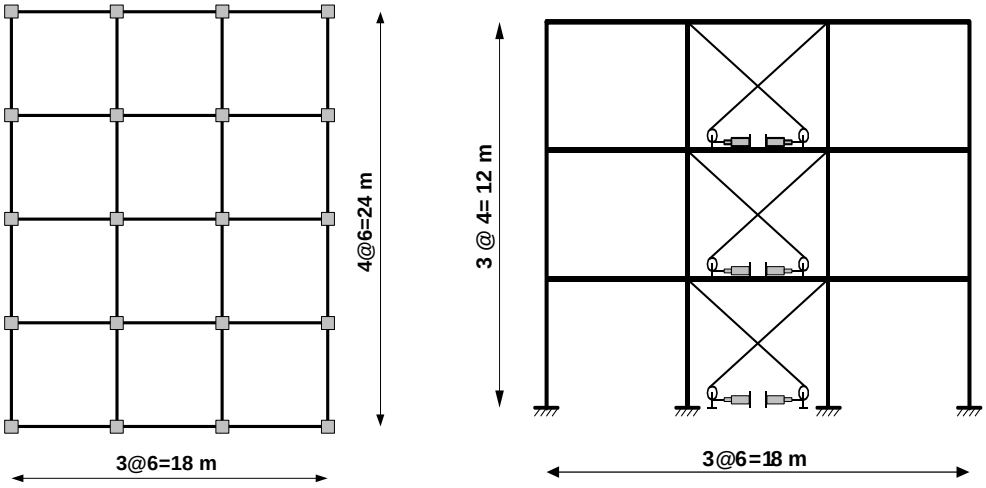

Figure 3 Floor and elevation views of 3-storey reinforced concrete building

The structure was analyzed in the short direction, under the N-S component of 1940 El Centro earthquake record, with and without active control. The frames were equipped with control hardware, as illustrated in Figure 3. Different c/r ratios were used to establish an optimum value. The results are plotted in Figures 4 through 6. Figure 4 illustrates the effect of c/r ratio on the reduction of lateral displacements. It becomes clear from this figure that Pattern 1 provides the highest control, reducing the maximum horizontal roof displacement by approximately 70%. This is attained at a c/r ratio of $1x10^7$ [log(c/r) = 7]. Figure 5 shows time histories for one of the control forces at the first storey level for two analyses with two different values of c/r ratio; i) log(c/r) = 7 and ii) log(c/r) = 10. Though the level of control force is significantly higher when log(c/r) = 10 was used, no further reduction is attained in roof displacements. Figure 6 illustrates the time history of control achieved in roof displacements throughout the entire duration of the most intense segment of earthquake record.

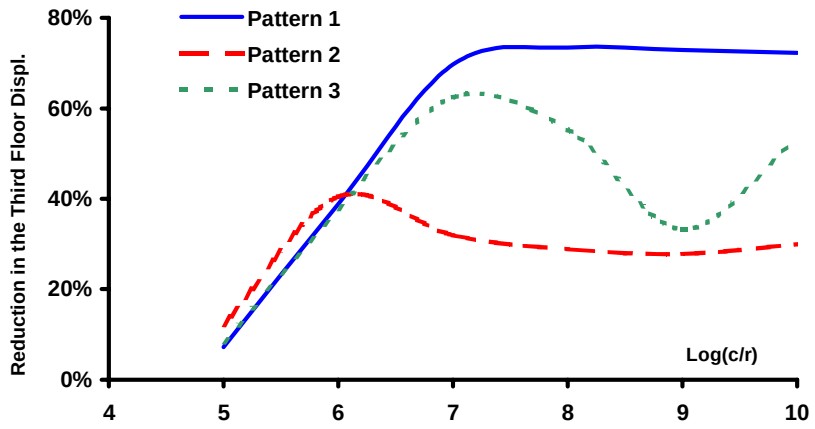

Figure 4 The effect of c/r ratio on reduction in lateral displacements

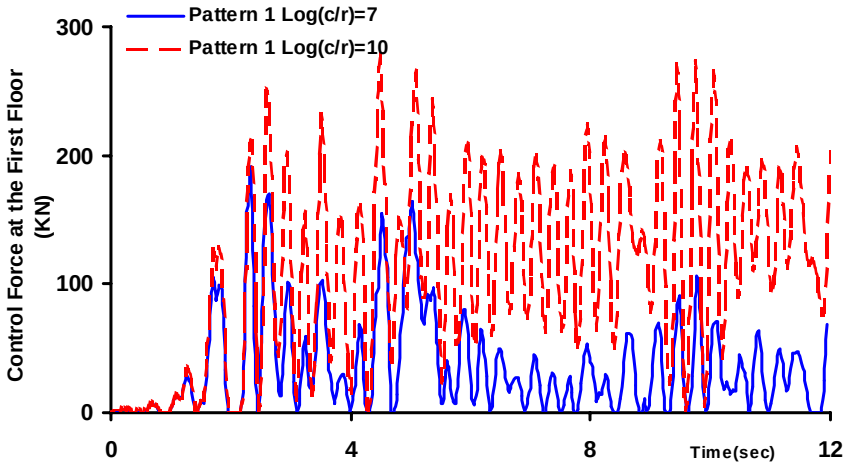

Figure 5 Variation of control force with c/r ratio

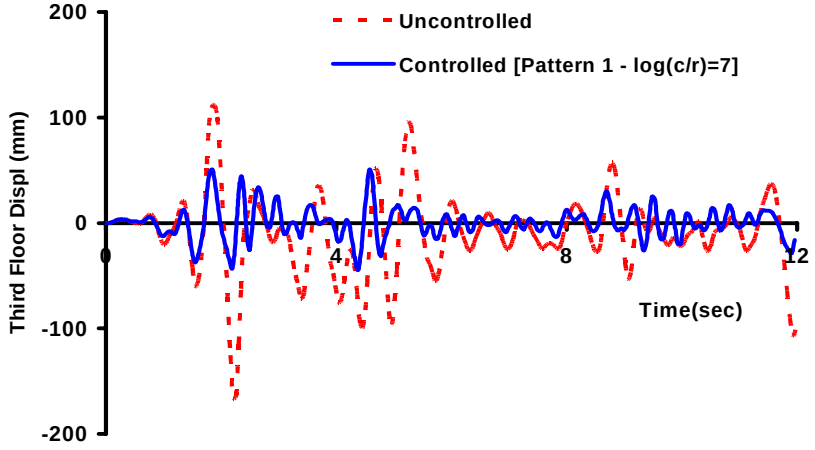

Figure 6 Roof displacement of the 3-storey frame as affected by active control

An important aspect of seismic control in frames is the reduction in inter-storey drift to prevent damage to nonductile columns. Maximum inter-storey drift is plotted in Figure 7 for uncontrolled and controlled structures based on the optimum value of c/r = 1.0 x 10^7. The results show that Patterns 1 and 3 were able to provide reasonable levels of inter-storey drift control, whereas, Pattern 2, with control forces limited to the first floor, was not able to control the storey drift in upper stories. The control of inter-storey drift in the first and second stories, where high values of inter-storey drift is experienced, is illustrated in Figures 8 and 9, respectively, during the entire duration of the earthquake record.

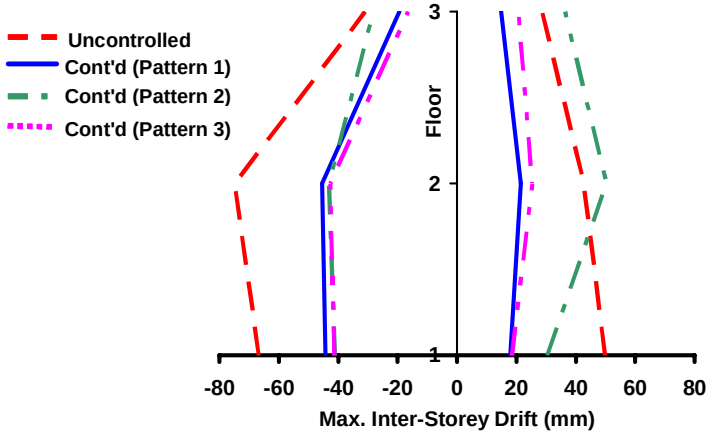

Figure 7 Inter-storey drift control in the 3-storey building

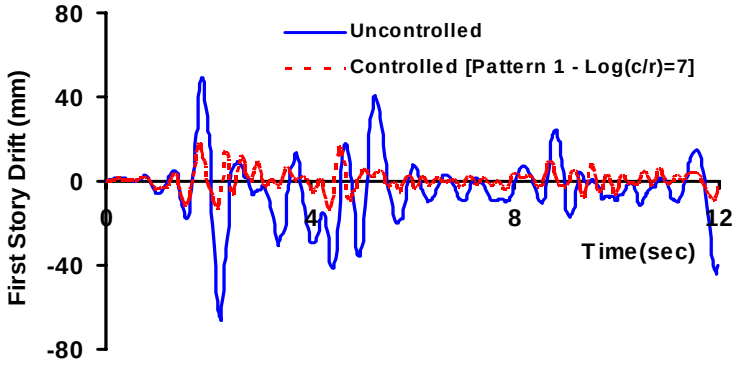

Figure 8 Control of inter-storey-drift at the first floor of 3-storey frame

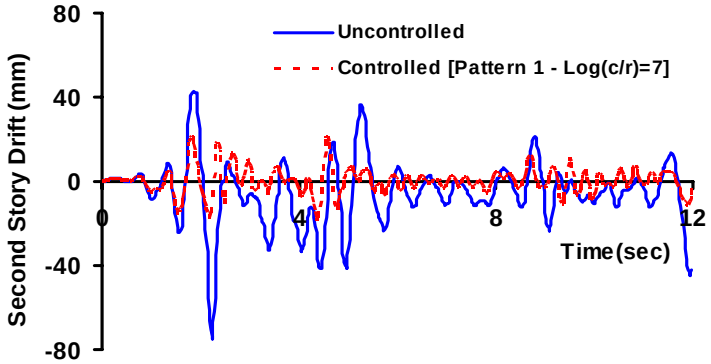

Figure 9 Control of inter-storey drift at the second floor of 3-storey frame

Five-Story Reinforced Concrete Frame Structure

A five-storey concrete building was designed using the provisions of the National Building Code of Canada [7]. The floor plan was the same as the 3-storey building considered earlier, and shown in Figure 3(a). Two different arrangements of control forces were applied as illustrated in Figure 10. Pattern 1 provided lateral bracing in the middle bay, along the entire height of the frame. Pattern 2 provided bracing within the bottom three stories, extending over three bays, as shown in Figure 10(b).

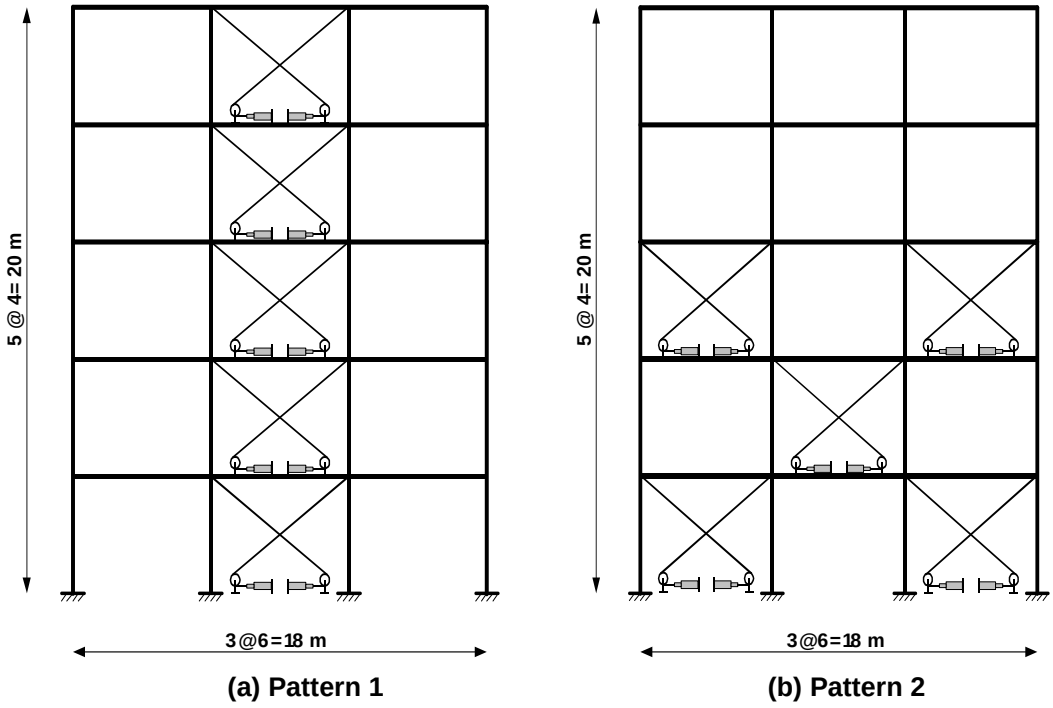

Figure 10 Patterns of control forces considered

The structure was analyzed in the short direction under the N-S component of 1940 El Centro earthquake record, with and without active control. The frames were equipped with the control hardware illustrated in Figure 10. Different c/r ratios were used to establish an optimum value. Figures 11 and 12 indicate that the optimum value for c/r ratio was log(c/r) = 7, beyond which there was not much improvement in deformation reduction, though control forces kept increasing. Figure 13 shows storey drift control attained by the two force patterns considered. It is clear from this figure that Pattern 1 provided a better control of inter-storey drift and associated damage to the frame elements. Time histories for the roof displacement, as well as inter-storey drift control at first and second floors, are illustrated in Figures 14 through 16.

An important aspect of the active control procedure presented in this paper is its applicability to reinforced concrete structures in the inelastic range of deformations. Inelastic deformations were introduced through a hysteretic model. The effect of active control on member end hysteretic relationship is illustrated in Figures 17 and 18. Figure 17 shows the moment-chord angle hysteretic relationship for a first-storey column of the 5-storey frame analyzed, with and without control. The column developed a displacement ductility ratio of 5.8 in the absence of control and showed a reduced ductility demand of 2.3 when seismic control was activated. Similarly, the second storey beam, which was one of the critical beams of the 5-storey frame, developed a reduction in the beam ductility demand from 2.0 to 1.2 due to active control.

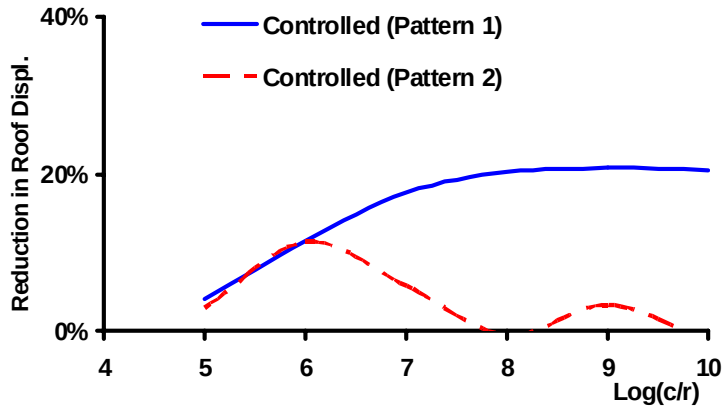

Figure 11 Reduction in roof displacement as affected by c/r ratio

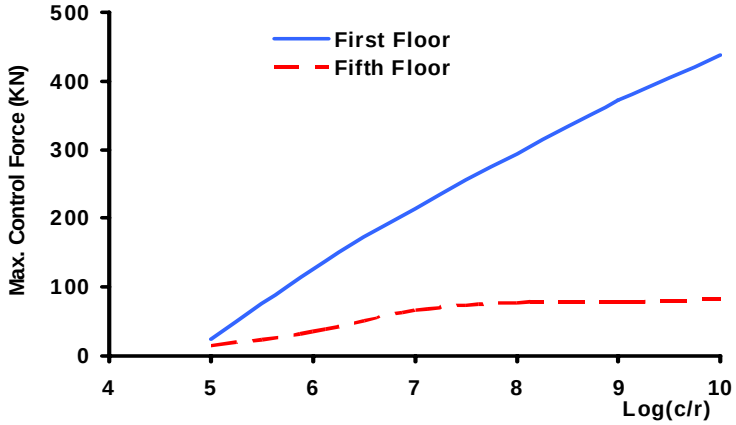

Figure 12 Maximum control force as affected by c/r ratio

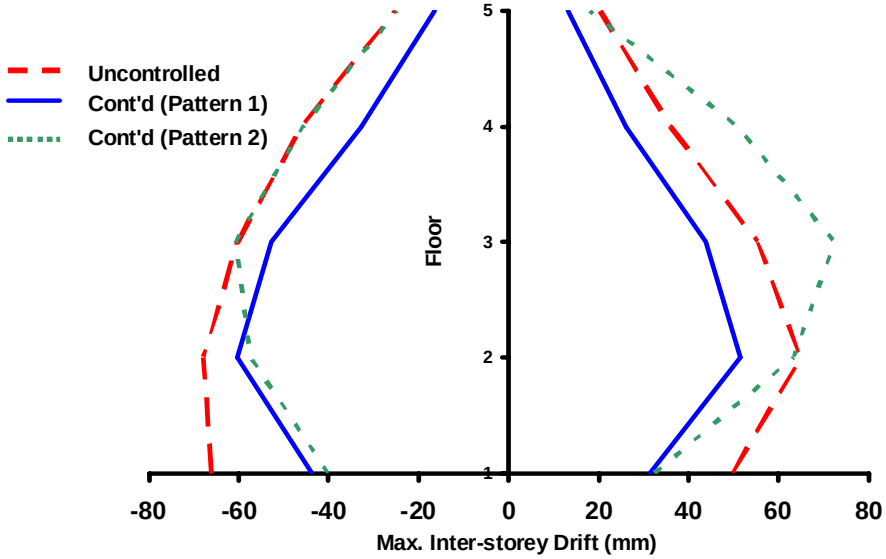

Figure 13 Inter-storey drift control in 5-storey building

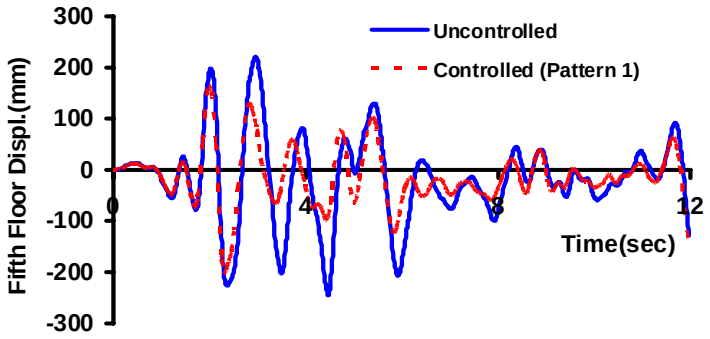

Figure 14 Roof displacement as affected by active control

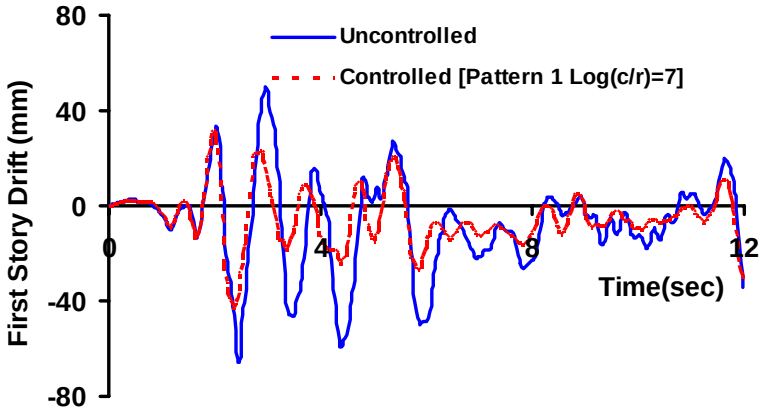

Figure 15 Control of inter-storey-drift at the first floor of 5-storey frame

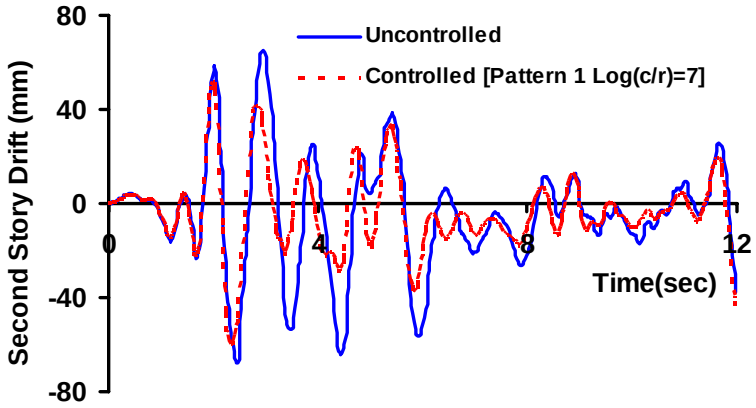

Figure 16 Control of inter-storey-drift at the second floor of 5-storey frame

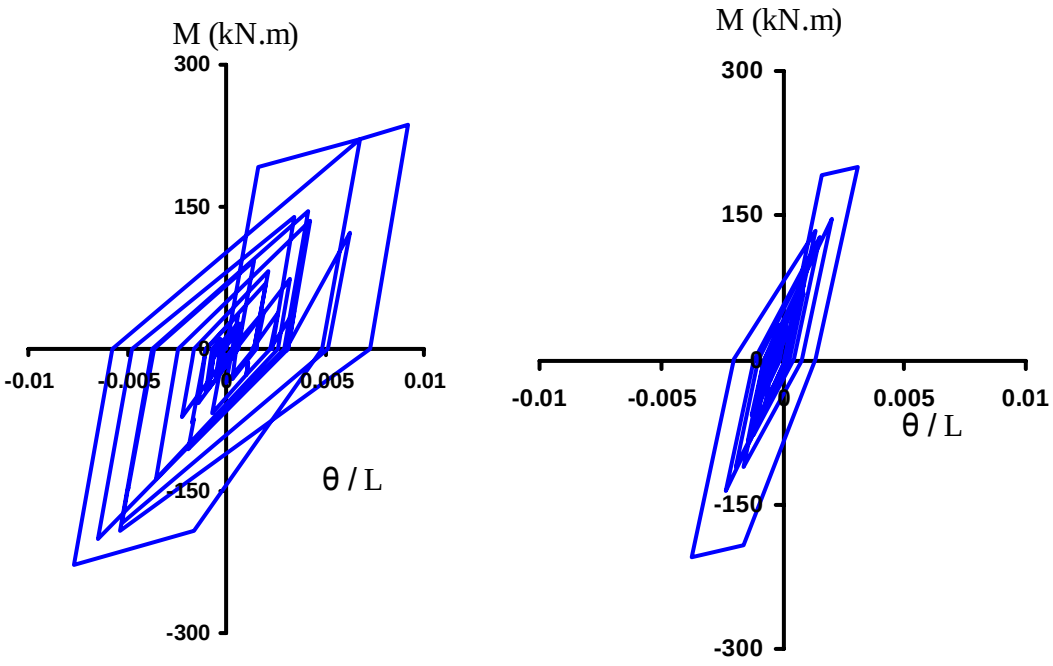

a) Without control b) With control

Figure 17 Hysteretic behavior of a first-storey column

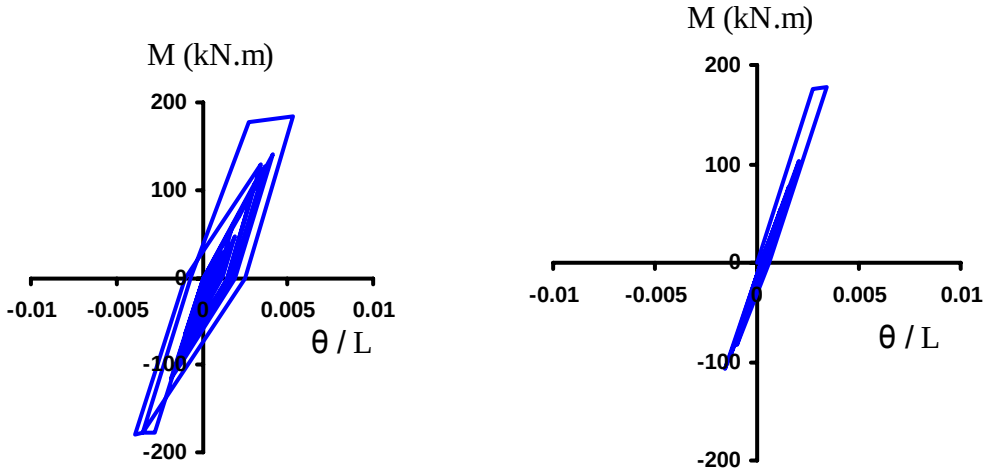

a) Without control b) With optimum control

Figure 18 Hysteretic behavior of a 2nd storey beam

CONCLUSIONS

The following conclusions can be drawn from the analytical research presented in this paper:

- The active control technique presented in the paper can be used effectively to reduce seismic displacement and ductility demands. The reinforced concrete frame structures analyzed in this

investigation showed approximately 1/3 to 2/3 reductions in inter-storey drift due to active control. This was accompanied by similar reductions in ductility demands.

- There is an optimum level of diagonal control force that produces the maximum reduction in horizontal displacements. Further increase or decrease in control forces may result in reduced effectiveness, accompanied by increased horizontal displacements.
- Arrangement of control forces in a frame structure plays an important role on the effectiveness of control process. Diagonal tension forces applied within a bay, along the entire height of the building, appear to provide the most effective control pattern under seismic excitations.

REFERENCES

1. Takeda,T., Sozen,M.A. and Nielson,N.N. “Reinforced Concrete Response to Simulated Earthquake.” Journal of the Structural Division, ASCE, Vol.96, No.ST12, December 1970, pp.2557-2573.
2. Soong,T.T. “Active Structural Control in Civil Engineering.” Technical Report, NCEER-87-0023, Nov. 1987.
3. Chung, LL. Lin, R.C. Soong, T.T. and Reinhorn, A.M. "Experimental Study of Active Control of MDOF Structures Under Seismic Excitation." Technical Report NCEER-88-0025, July 1988.
4. Holzer,S.M. “ComputerAnalysis of Strructures.” Elsevier, New York, 1985, p 426.
5. Lin, R.C., Soong,T.T. and Reinhorn A.M. “Experimental Evaluation of Instantaneous Optimal Algorithms for Structural Control.” Technical Report, NCEER-87-0002, April 1987.
6. Soong, T. T. “Active Structural Control, Theory & Practice.” Longman Group UK Limited, 1990, p194.
7. NBCC-1995, “National Building Code of Canada.” National Research Council of Canada, Ottawa, Ontario, 1996.